Mesoscopic dynamics of diffusion-influenced enzyme kinetics

Jiang-Xing Chen[a] and Raymond Kapral[b]
Chemical Physics Theory Group, Department of Chemistry, University of Toronto, Toronto, Ontario M5S 3H6, Canada

(Received 3 September 2010; accepted 27 November 2010; published online 24 January 2011)

A particle-based mesoscopic model for enzyme kinetics is constructed and used to investigate the influence of diffusion on the reactive dynamics. Enzymes and enzyme-substrate complexes are modeled as finite-size soft spherical particles, while substrate, product, and solvent molecules are point particles. The system is evolved using a hybrid molecular dynamics–multiparticle collision dynamics scheme. Both the nonreactive and reactive dynamics are constructed to satisfy mass, momentum, and energy conservation laws, and reversible reaction steps satisfy detailed balance. Hydrodynamic interactions among the enzymes and complexes are automatically accounted for in the dynamics. Diffusion manifests itself in various ways, notably in power-law behavior in the evolution of the species concentrations. In accord with earlier investigations, regimes where the product production rate exhibits either monotonic or nonmonotonic behavior as a function of time are found. In addition, the species concentrations display both $t^{-1/2}$ and $t^{-3/2}$ power-law behavior, depending on the dynamical regime under investigation. For high enzyme volume fractions, cooperative effects influence the enzyme kinetics. The time dependent rate coefficient determined from the mass action rate law is computed and shown to depend on the enzyme concentration. Lifetime distributions of substrate molecules newly released in complex dissociation events are determined and shown to have either a power-law form for rebinding to the same enzyme from which they were released or an exponential form for rebinding to different enzymes. The model can be used and extended to explore a variety of issues related concentration effects and diffusion on enzyme kinetics. © *2011 American Institute of Physics*. [doi:10.1063/1.3528004]

I. INTRODUCTION

Diffusion-controlled reactions have been studied extensively and are one of the central topics in chemical and biological reaction kinetics. The well-known enzyme-catalyzed Michaelis–Menten (MM) reaction,[1]

$$E + S \underset{k_{-1}}{\overset{k_1}{\rightleftharpoons}} C \overset{k_{cat}}{\rightarrow} E + P, \tag{1}$$

is a standard model in this field. Here E, S, C, and P represent the enzyme, substrate, enzyme–substrate complex, and product, respectively. The phenomenological rate constants for the various reaction steps are k_1, k_{-1}, and $k_{\rm cat}$.

The classical mean-field description of MM kinetics assumes that diffusion is fast compared to reaction and ignores many-body competition effects. For fast reactions, diffusion shapes the spatial distribution of reactants, leading to spatial and temporal inhomogeneous concentration profiles near the enzymes. The existence of spatial concentration fluctuations occurring on different time scales leads to rich dynamical behavior in diffusion-influenced reactions. It is well known that reaction rate coefficients can be controlled by diffusion[2] and can become time dependent as a result of diffusion effects.[3–5] The final approach of reactant concentrations to equilibrium is determined by diffusion and leads to a power-law decay instead of exponential relaxation.

The nonuniform distribution of substrates and products can induce correlations among enzymes, which may play an important role in the dynamics. For example, molecular synchronization waves in arrays of allosterically regulated enzymes have been suggested to arise as a result of coherence of catalytic turnover cycles of individual enzymes induced by diffusing product molecules.[6] Even the simplest reaction–diffusion systems with only two-body reactions and no autocatalysis show very rich and incompletely understood phenomena. Investigations of the breakdown of classical descriptions of MM kinetics require theoretical tools that can probe diverse space and time scales and can account for fluctuations. A variety of theoretical,[7–22] simulation,[18–29] and experimental[30–33] studies have been used successfully to study a range of problems in this area.

To simplify this complicated problem, a single enzyme is usually considered and enzymes are assumed to be static. These assumptions may not always be valid. Once a substrate or product is released from a complex, it may diffuse and rebind with other enzymes, giving rise to cooperative enzyme reactions. The mobility of enzymes can lead to new interactions among them as the enzymes move into and out of the range of the potential, which may affect dynamical behavior.[27,34] Hydrodynamic interactions are long ranged and can influence enzyme motions.[34] Therefore, the assumptions that enzymes act independently or are immobile may neglect important correlations.

[a]Electronic mail: jchen@chem.utoronto.ca.
[b]Electronic mail: rkapral@chem.utoronto.ca.

Since such complex many-body problems cannot be solved exactly, theoretical treatments must rely on approximations to the reactive dynamics. Consequently, it is of interest to develop simulation schemes that are able to describe reaction–diffusion induced correlations, fluctuations, and hydrodynamic interactions. Such methods can provide additional insights into the dynamical behavior of these systems and be used to test the applicability of other theoretical models.

In this paper, we construct a simple mesoscopic model for MM kinetics, which is based on a hybrid molecular dynamics–multiparticle collision (MD–MPC) dynamics for the time evolution of the reactive species and solvent molecules.[35,36] We focus on the influence of diffusion on the reaction dynamics and cooperative effects involving the interactions among many enzyme molecules. The paper is organized as follows. In Sec. II, the mesoscopic MM model is introduced. In this section both nonreactive and reactive collision dynamics that preserve mass, momentum, and energy are described. Details related to the simulation of the mesoscopic dynamics are given in Sec. III. In this section the simulation results are also presented and discussed. Section IV presents results for systems where the volume fraction of enzymes and complexes is high. The conclusions of this investigation are given in Sec. V.

II. MESOSCOPIC ENZYMATIC REACTION DYNAMICS

We now describe how a coarse-grain model of a system in which Michaelis–Menten-type enzymatic reactions take place can be constructed. Our mesoscopic model preserves important general features of full molecular dynamics, such as the basic mass, momentum, and energy conservation laws but eliminates fine details of both nonreactive and reactive collision events. The simplification of the dynamics allows us to carry out long-time simulations of the reactive dynamics for large systems. Through the use of such a mesoscopic model, we can investigate the influence of diffusion on the reaction dynamics and cooperative effects involving the interactions among many enzymes. Because our dynamics preserves the basic conservation laws, hydrodynamic interactions are properly accounted for and no additional assumptions about friction coefficients or random forces need be made.

We consider a system comprising reactive E, S, C, and P species, as well as a large excess of nonreactive solvent molecules M that serve as heat bath. The reactive species are idealized as structureless particles in order to coarse grain over the details of the molecular structure and catalytic process, such as internal conformational changes in the enzyme and specific aspects of bond-making and bond-breaking events. The large enzyme and enzyme–substrate molecules are treated as finite-size particles while all other species, substrate, product, and solvent molecules are taken to be point particles. An instantaneous configuration of the system showing these species (with the exception of the large number of solvent molecules) is given in Fig. 1.

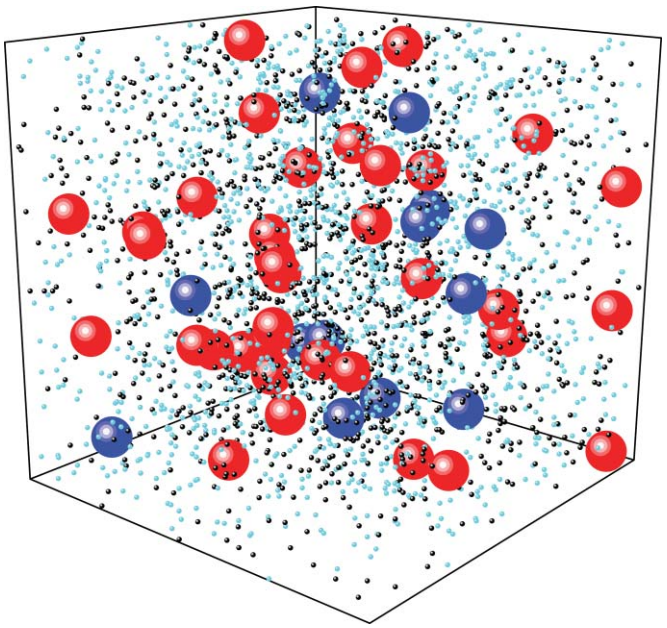

FIG. 1. Instantaneous configuration of the system containing enzymes (red spheres), enzyme–substrate complexes (blue spheres), substrates (black dots), and products (cyan dots). Solvent molecules are not shown.

A. Nonreactive dynamics

The nonreactive dynamics is described by hybrid molecular dynamics–multiparticle collision dynamics.[35–38] In this scheme the enzymes and enzyme–substrate complexes interact with each other and with the solvent, substrate, and product molecules through repulsive Lennard-Jones (LJ) potentials,

$$V_{\mathrm{LJ}}(r) = 4\epsilon_\nu\left[\left(\frac{\sigma_\nu}{r}\right)^{12} - \left(\frac{\sigma_\nu}{r}\right)^{6} + \frac{1}{4}\right], \quad r < r_c, \tag{2}$$

and zero otherwise. Here, $r_c = 2^{1/6}\sigma_\nu$ is a cutoff distance and ν labels the type of interaction. The total potential energy for a system with N_E enzyme molecules with coordinates $\mathbf{r}^{N_E} = (\mathbf{r}_1, \mathbf{r}_2, \ldots, \mathbf{r}_{N_E})$, with similar expressions for the other species, is given by

$$\begin{aligned}\mathcal{V}(\mathbf{r}^{N_E}, \mathbf{r}^{N_C}, \mathbf{r}^{N_S}, \mathbf{r}^{N_P}, \mathbf{r}^{N_M}) \\ = \mathcal{V}_{EE} + \mathcal{V}_{EC} + \mathcal{V}_{CC} + \mathcal{V}_{ES} + \mathcal{V}_{EP} + \mathcal{V}_{EM} \\ + \mathcal{V}_{CS} + \mathcal{V}_{CP} + \mathcal{V}_{CM},\end{aligned} \tag{3}$$

where the subscripts indicate the type of interaction. There are no interaction potentials among the solvent, substrate, or product molecules. These interactions are described by multiparticle collisions discussed below. The mesoscopic dynamics consists of concatenations of two steps: (1) Newtonian evolution of all species governed by the potential $\mathcal{V}$. This is the MD step of the algorithm. (2) Multiparticle collisions among the S, P, and M species occur at discrete time intervals τ. In order to carry out the multiparticle collisions, the system is partitioned into cells ξ and rotation operators $\hat{\omega}_\xi$, chosen from some set of rotation operators, are assigned to each cell. For cell ξ the center of mass velocity $\mathbf{V}_\xi$ is computed and the postcollision velocity of the particle i in the cell is given by

$$\mathbf{v}_i' = \mathbf{V}_\xi + \hat{\omega}_\xi(\mathbf{v}_i - \mathbf{V}_\xi). \tag{4}$$

This simple collision dynamics mimics the net effects of many real collisions that occur in the time interval τ. MD–MPC dynamics conserves mass, momentum, and energy as well as phase space volumes. Thus, it has many of the important characteristics of full molecular dynamics but is computationally efficient since there are no forces among the majority of the particles in the system. The transport properties of the solvent undergoing MPC dynamics can be computed analytically.[35,36,39–41] Reviews of this method which contain additional details concerning the theory, simulation methods, and applications are given in Refs. 37 and 38.

B. Reactive dynamics

The reaction dynamics is also described at a mesoscopic level that preserves the essential features of full molecular dynamics. Reactive collisions are constructed to conserve mass, momentum, and energy and account for energy transfers to and from the surrounding solvent molecules that serve as heat bath. Earlier, reactive MPC models considered simple catalytic interconversion between two species[42] or highly coarse grained bulk reactive dynamics.[43] The complex formation and dissociation reactions involving finite-size species considered here require a new set of reactive collision rules to ensure that the conservation laws are satisfied.

Enzyme catalysis involves a number of processes that depend on the detailed structure and dynamics of the protein, substrate, and product molecules. Typically, the substrate diffuses to the vicinity of the active site of the protein where it binds to form the enzyme–substrate complex. This often then induces conformational changes in the enzyme–substrate complex that lead to a chemical reaction that produces product, which then dissociates from the complex to regenerate the enzyme. The bond-making and bond-breaking events, as well as the conformational transformations in the protein and reactive event, involve substantial energy changes. This energy is ultimately dissipated by the surrounding solvent medium. Thus, a full description of such dynamics requires a microscopic, or finer mesoscopic, level of detail.[44]

Our mesoscopic description of enzyme kinetics does not attempt to describe this level of detail. Instead it focuses on the diffusive dynamics leading to the formation of the enzyme–substrate complex and the subsequent dissociation of the complex to form either substrate or product. All microscopic details described above are subsumed in simple reactive collision events characterized by reaction rates that, nevertheless, account for the net energy changes with the environment in which the reactions take place. Such a coarse description allows us to study the effects of diffusion on the enzyme kinetics in some detail and also consider cooperative reaction and diffusion effects in ensembles of enzyme molecules. Below we show how the main reactive events can be described at a mesoscopic level. Full details are presented in Appendix.

1. Formation of enzyme-substrate complex: $E + S \rightarrow C$

The enzyme and substrate diffuse in the solvent until they encounter each other. The substrate must find the active region on the enzyme before the catalytic reaction can commence. While our model can be generalized to account for an active domain on the surface of the enzyme, here we model this effect by carrying out the reactive collision with probability p on encounter. It is possible that more than one substrate will enter the reaction zone of the enzyme in a given time interval and we must account for this possibility as well. More specifically, once n substrate molecules enter into the radial reaction region $r < r_c$ of an enzyme for the first time, the probability of reaction is $p_R = 1 - (1 - p)^n$. If the substrates do not react with the enzyme at the first MD time step as a consequence of a small reaction probability p (or small n) when they enter in the reaction region, they lose the opportunity to react until they enter into the region from outside again. One of the n substrates is randomly selected for possible reaction. A random number in [0,1) is chosen and if it is smaller than p_R the reaction $E + S \rightarrow C$ occurs.

The velocity of the newly formed complex, $\mathbf{v}_C'$, is taken to be equal to the center of mass velocity of the enzyme and the substrate molecule that participates in the reaction:

$$\mathbf{v}_C' = \mathbf{V}_{ES} = \frac{m_E \mathbf{v}_E + m_S \mathbf{v}_S}{m_C}, \tag{5}$$

where the mass of the complex is $m_C = m_E + m_S$. The relative energy of the colliding pair is ultimately dissipated in the environment and to take this into account we change the velocities of neighboring solvent molecules. The manner in which this is done for an arbitrary number of participating solvent molecules so that the basic conservation laws are preserved is described in Appendix. Here it is sufficient to imagine that only two neighboring solvent molecules $M1$ and $M2$ participate in this event and in this case the general formulas derived in Appendix reduce to the following expression for their postreaction velocities:

$$\begin{aligned} \mathbf{v}_{M1}' &= \tfrac{1}{2}(\mathbf{v}_{M1} + \mathbf{v}_{M2}) + \tfrac{1}{2}\hat{\mathbf{n}}_1 v_{Mr}' \\ \mathbf{v}_{M2}' &= \tfrac{1}{2}(\mathbf{v}_{M1} + \mathbf{v}_{M2}) - \tfrac{1}{2}\hat{\mathbf{n}}_1 v_{Mr}', \end{aligned} \tag{6}$$

where

$$v_{Mr}' = \left(\frac{2\mu_{ES}}{m_M} v_r^2 + \frac{4}{m_M}\mathcal{V}_{ES}(r_{ES}) + v_{Mr}^2\right)^{1/2}. \tag{7}$$

Here $\mathbf{v}_{Mr} = \mathbf{v}_{M1} - \mathbf{v}_{M2}$ is the relative velocity of the two solvent molecules, $\hat{\mathbf{n}}_1$ is a randomly chosen unit vector, $\mathbf{v}_r = \mathbf{v}_E - \mathbf{v}_S$, $\mathbf{r}_{ES} = \mathbf{r}_E - \mathbf{r}_S$, and μ_{ES} is the reduced mass of E and S. It is easy to verify that with this choice of postreaction velocities mass, momentum, and energy are conserved in the reaction leading to complex formation.

2. Dissociation of enzyme-substrate complex: $E + S \leftarrow C \rightarrow E + P$

Once a complex is formed it may either dissociate to release the substrate or the catalytic reaction can occur with production of the product molecule. To account for these reactions, we assume that the lifetimes of the complex before dissociation, t_d, are exponentially distributed, although other distributions may be chosen to account for more specific product release mechanisms. The probability that no reaction occurs in the time interval t_d is $p_d(t_d) = \exp(-(k_{-1}^0 + k_{\text{cat}})t_d)$.

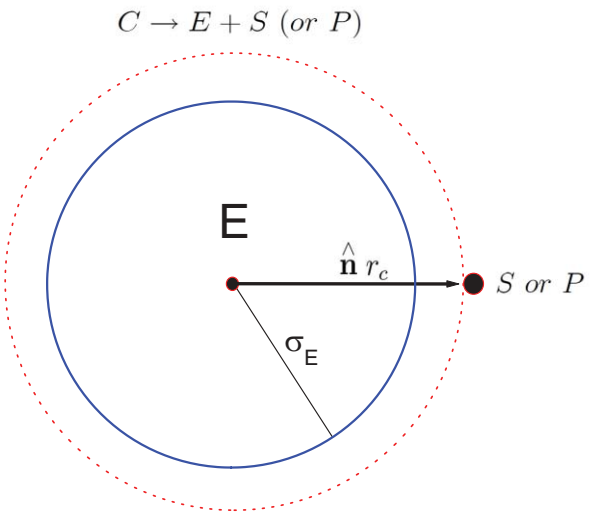

FIG. 2. Schematic representation of the dissociation C → E+S (or P).

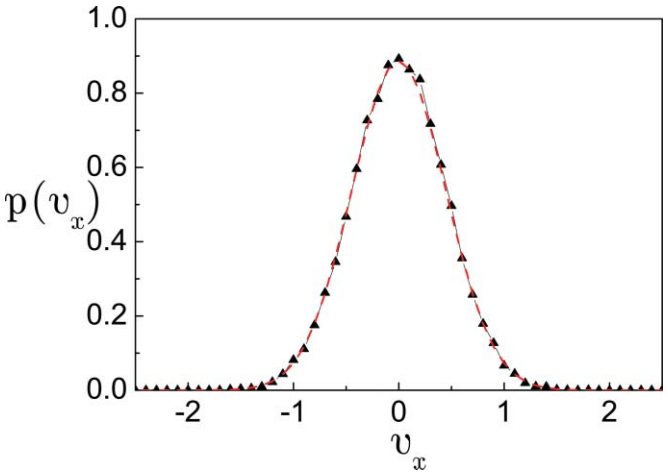

FIG. 3. Velocity distribution of newly formed substrate molecules that result from dissociation of the enzyme–substrate complex (solid triangles). The simulation results are compared with a Maxwell–Boltzmann distribution with $k_BT = 0.2$ (solid line). The simulation parameters: $N_E(0) = 200$, $N_S(0) = 6000$, $\sigma_E = 3.0$, $k_BT = 0.2$, and $k_{-1} = 0.015$.

Here k_{-1}^0 and $k_{\rm cat}$ are the intrinsic dissociation rate constants for substrate and product, respectively. If the complex is formed at time t, the time of the next dissociation, $t + t_d$ can be computed from $t + 1/(k_{\rm cat} + k_{-1}^0)\ln(1/r_1)$, where r_1 is random number chosen from a uniform distribution on the interval [0,1). Given another random number r_2 on [0,1), the reaction $C \to E + P$ will occur if $r_2 < k_{\rm cat}/(k_{\rm cat} + k_{-1}^0)$, otherwise the reaction is $C \to E + S$ will take place.

We assume that the newly formed S or P molecules appear at a distance $\mathbf{r}_{S(P)} = \mathbf{r}_C + \hat{\mathbf{n}}r_c$, where $\hat{\mathbf{n}}$ is a randomly oriented radial unit vector (see sketch in Fig. 2), which is outside the range of the potential acting between E and either S or P. (It is not necessary to assume that S or P appear at a distance outside the range of the potential but this simplifies the computation of the postreaction velocities.) Energy is taken from the environment to affect the dissociation reactions. Once again we consider the simple case where two neighboring solvent molecules supply this energy from their relative motion. Thus, the postreaction velocities are taken to be (see Appendix)

$$\mathbf{v}'_{Mj} = \tfrac{1}{2}(\mathbf{v}_{M1} + \mathbf{v}_{M2}),\ j = 1, 2, \tag{8}$$

for the solvent molecules and

$$\begin{aligned} \mathbf{v}'_E &= \mathbf{v}_C + \frac{m_S}{m_C}\sqrt{\frac{m_M}{2\mu_{ES}}}\hat{\mathbf{r}}_{SE}v_{Mr}, \\ \mathbf{v}'_S &= \mathbf{v}_C - \frac{m_E}{m_C}\sqrt{\frac{m_M}{2\mu_{ES}}}\hat{\mathbf{r}}_{SE}v_{Mr}, \end{aligned} \tag{9}$$

for the enzyme and substrate molecules. Here $\hat{\mathbf{r}}_{SE}$ is a unit vector pointing from E to S.

When dissociation of the complex occurs, the postreaction velocity of the substrate is determined by the velocities of the neighboring solvent molecules that participate in the energy exchanges that occur during reaction. In Fig. 3, we show the velocity distribution of the newly formed substrate molecules as a result of the complex dissociation. These results show that a Maxwell–Boltzmann distribution, characterized by the temperature of the system, is obtained. Since solvent molecule thermal equilibrium is rapidly established on the slower time scale of reactive events, the newly formed substrate molecule velocities reflect this rapid solvent equilibration process and exhibit an equilibrium velocity distribution. Similar expressions apply for product formation[45] where S is replaced by P. As for nonreactive dynamics, this reactive collision dynamics conserves mass, momentum, and energy. A more general treatment of such dissociation reactions is given in Appendix.

When the reactive collision events for binding of the substrate to the enzyme to form the complex and dissociation of the complex to regenerate the substrate and enzyme are combined with multiparticle collisions, this reversible kinetics satisfies detailed balance.

III. SIMULATION OF ENZYME CATALYSIS

A. Simulation details

Our simulations of the enzyme kinetics were carried out in a cubic box with sides $L = 60$ and periodic boundary conditions. The enzyme molecules were first placed in the box with randomly chosen positions, avoiding overlapping configurations. The pointlike substrate and solvent particles were then randomly assigned positions that were within the cube but outside the enzyme spheres so that the initial potential energy is zero. When necessary, the nonreactive dynamics is then simulated to further equilibrate the initial configuration.

In order to perform multiparticle collisions, the box was subdivided into $L^3 = 60^3$ cells with length $a_0 = 1$. The average number density of solvent molecules per cell was $n_M = 8$ so that there were on average 1.728×10^6 solvent molecules in the box. Velocity rotations by $\pi/2$ about randomly chosen axes were carried out in the multiparticle collision step. The masses of the S, P, and M species were taken to be identical and given by $m = 1$, while the mass of the enzyme was adjusted according to its volume to ensure that the enzyme is approximately neutrally buoyant. Random shifts of the grid defining the collision cells were also applied, so that

Galilean invariance is ensured.[37–39,46] The initial velocities of all molecules were chosen from a Maxwell–Boltzmann distribution characterized by the temperature T.

The LJ potentials describing the interactions between enzyme or complex and substrate, product and solvent molecules were characterized by an energy parameter $\epsilon_1 = 1.0$ and length parameter $\sigma_1 = \sigma_E = 3.0$. The cutoff distance is $r_c = 2^{1/6}\sigma_1$. The LJ potentials describing the $E-E$, $E-C$, and $C-C$ interactions have energy parameter $\epsilon_2 = 2.0$ and length parameter $\sigma_2 = 6.2$. All quantities in the paper were reported in dimensionless units based on energy ϵ_1, mass m, and cell length a_0 parameters: $r/a_0 \to r$, $t(\epsilon_1/m/a_0^2)^{1/2} \to t$ and $k_BT/\epsilon_1 \to T$. The MD time step used to integrate Newton's equations of motion with the velocity Verlet algorithm was $\Delta t = 0.005$. Multiparticle collisions were carried out every 200 MD steps so that $\tau = 1$.

While the enzyme and complex molecules experience soft LJ interactions with the point particle species and each other in theoretical estimates given below, it is useful to define an approximate enzyme size to account for reactive collisions with substrate molecules and to estimate enzyme diffusion coefficients and volume fractions. Since the point particles interact with the enzymes with a repulsive LJ potential with length parameter σ_E, and the potential range is $r_c = 2^{1/6}\sigma_E$, this is an appropriate value to take for the enzyme radius in its interactions with the solvent, substrate, and product molecules (see Fig. 2). The mass of a neutrally buoyant enzyme molecule was then taken to be $m_E \approx 4\pi r_c^3 n_M/3$, where n_M is the number density of solvent molecules.

B. Michaelis–Menten kinetics

There are numerous theoretical studies of the influence of diffusion on enzyme kinetics, which make various predictions for rate constants or time evolution of concentrations. These investigations range from those based on diffusion or Brownian motion models to kinetic theory and molecular dynamics descriptions. Although our model is mesoscopic in character, in contrast to most other approaches with the exception of full molecular dynamics, it is a particle-based scheme that explicitly accounts for all species, including solvent, and preserves all conservation laws. Consequently, it can be used to test the validity of simpler theories that coarse grain over some of these degrees of freedom or make other simplifying assumptions to obtain the results.

For the enzyme catalyzed reaction,

$$E + S \underset{k_{-1}}{\overset{k_1}{\rightleftharpoons}} C \overset{k_{\rm cat}}{\to} E + P,$$

the production rate of product P, $\nu(t)$, is given by

$$\nu(t) = \frac{d[P(t)]}{dt} = k_{\rm cat}[C(t)], \tag{10}$$

where $[\alpha] = N_\alpha/V$ is the number density of species α. The maximum production rate occurs when all of the enzyme exists in the form of the enzyme–substrate complex so that $[C] = [E(0)] \equiv [E_0]$ and $\nu_{\max} = k_{\rm cat}[E_0]$.

Standard treatments of MM kinetics assume mean-field kinetic equations where the rate constants k_1 and k_{-1} have their intrinsic values, k_1^0 and k_{-1}^0, respectively, and make use of a steady state approximation on the rate of complex formation to give

$$[C(t)] = [C]_{ss}\left(1 - e^{-(k_1^0[S_0]+k_{-1}^0+k_{\rm cat})t}\right), \tag{11}$$

for the pseudo-first-order condition where $[S] \approx [S_0] \gg [E_0]$. The time dependent production rate in this approximation is denoted by $\nu^0(t)$. The steady state concentration of complex is $[C]_{ss} = [E_0][S_0]/(K_M^0 + [S_0])$, with $K_M^0 = (k_{-1}^0 + k_{\rm cat})/k_1^0$ the Michaelis constant. The steady state production rate then has the form, $\nu_{ss}^0 = k_{\rm cat}[E_0][S_0]/(K_M^0 + [S_0])$.

Within such a framework, diffusion effects may be taken into account approximately through the modification of the intrinsic reaction rate constants by diffusion so that[47] $k_1^D = k_1^0 k_D/(k_1^0 + k_D)$ and $k_{-1}^D = k_{-1}^0 k_D/(k_1^0 + k_D)$, where the Smoluchowski rate constant is $k_D = 4\pi D\bar{\sigma}_E$ with $D = D_E + D_S$ the mean diffusion coefficient of the enzyme and substrate molecules and $\bar{\sigma}_E$ an effective enzyme radius where the reactive boundary condition is applied in the solution of the diffusion equation. Using these forms, the Michaelis constant becomes $K_M^D = K_M^0 + k_{\rm cat}/k_D$. The time dependent production rate is $\nu^D(t)$ and the corresponding steady state production rate is $\nu_{ss}^D = k_{\rm cat}[E_0][S_0]/(K_M^D + [S_0])$. If diffusion effects are completely neglected then $K_M^D \to K_M^0$ and the steady state production rate adopt its earlier form $\nu_{ss}^D \to \nu_{ss}^0$.

It is well known that diffusion influences the nature of the time evolution of species concentrations and rate constants. In particular, the rate constant k_1, which characterizes the irreversible formation of the complex, $E + S \overset{k_1}{\to} C$ acquires time dependence. In the limit of low enzyme concentrations where all enzymes act independently and assuming diffusive dynamics, $k_1(t)$ has the form,[3–5]

$$k_1(t) = \frac{k_1^0 k_D}{k_1^0 + k_D} + \frac{(k_1^0)^2}{k_1^0 + k_D}\exp\left[\left(1 + \frac{k_1^0}{k_D}\right)^2 \frac{Dt}{\bar{\sigma}_E^2}\right] \times \operatorname{erfc}\left[\left(1 + \frac{k_1^0}{k_D}\right)\left(\frac{Dt}{\bar{\sigma}_E^2}\right)^{1/2}\right]. \tag{12}$$

This expression for $k_1(t)$ is obtained when the diffusion equation is solved subject to the radiation boundary condition, $k_1^0 n_S(\bar{\sigma}_E, t) = 4\pi\bar{\sigma}_E^2 D\hat{\mathbf{r}}\cdot\nabla n_S(\bar{\sigma}_E, t)$, where $n_S(r, t)$ is the local substrate density at a distance r from the enzyme and $\hat{\mathbf{r}}$ is unit radial vector. As noted earlier, k_1^0 is an intrinsic rate constant that characterizes reactive collision events in the diffusive boundary layer around the enzyme. Although the enzymes are soft spheres in our model, an estimate of k_1^0 can be obtained by supposing they are hard spheres and approximating the collision frequency of the enzyme and substrate molecules to give[42]

$$k_1^0 = p_R\left(\frac{8\pi k_B T}{\mu_{ES}}\right)^{1/2} r_c^2. \tag{13}$$

Since this intrinsic rate coefficient characterizes reactive events inside the diffusive boundary layer around the enzyme the radius $r_c = 2^{1/6}\sigma_E$ need not be the same as $\bar{\sigma}_E$ where the boundary condition on the diffusion equation is applied.

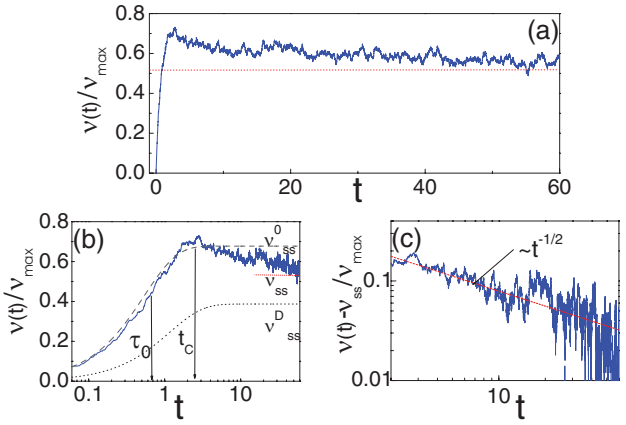

FIG. 4. (a) Plot of the production rate $\nu(t)/\nu_{\max}$ vs time. (b) Log-linear plot of $\nu(t)/\nu_{\max}$ vs time. The solid, dashed, and dotted curves correspond to $\nu(t)/\nu_{\max}$ from the simulation, $\nu^0(t)/\nu_{\max}$ and $\nu^D(t)/\nu_{\max}$, respectively. The vertical arrows indicate the characteristic times t_c and τ_0. The corresponding steady state values of ν^0_{ss}, ν^D_{ss}, and ν_{ss} are shown. (c) Fit of $(\nu(t)-\nu_{ss})/\nu_{\max}$ shows that the relaxation from the peak to the steady state value is governed by a power law with $t^{-1/2}$. The data are the result of an average over 16 realizations with different initial random configurations of enzymes. Simulation parameters: $N_E(0)=100$, $N_S(0)=10000$, $k_BT=0.2$, $\sigma_E=3.0$, $p_R=1.0$, $k^0_{-1}=0.1$, and $k_{\text{cat}}=0.5$.

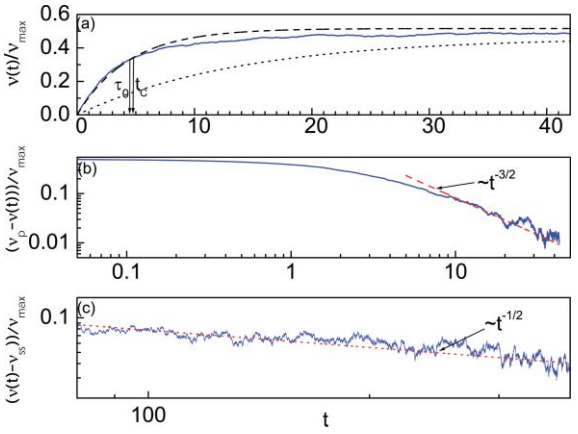

FIG. 5. (a) Plot of the production rate $\nu(t)/\nu_{\max}$ vs time. The solid, dashed, and dotted curves denote $\nu(t)/\nu_{\max}$ from the simulation, $\nu^0(t)/\nu_{\max}$ and $\nu^D(t)/\nu_{\max}$, respectively. The vertical arrows indicate the times t_c and τ_0. (b) Log–log plot $(\nu_P-\nu(t))/\nu_{\max}$ shows a $t^{-3/2}$ power-law behavior. The linear dotted line corresponds to $t^{-3/2}$ and is presented for comparison. (c) The log–log plot $(\nu(t)-\nu_{ss})/\nu_{\max}$ for long times indicates a $t^{-1/2}$ power-law decay to steady state. The data are an average of 32 realizations of the dynamics. Simulation parameters: $N_E(0)=100$, $N_S(0)=1000$, $k_BT=0.2$, $\sigma_E=3.0$, $p_R=1.0$, $k^0_{-1}=0.1$, and $k_{\text{cat}}=0.01$.

This rate coefficient can be determined by simulation and the validity approximate form can be tested.

Diffusion effects lead to power-law behavior of the concentrations, in contrast to that of classical kinetics where the production rate $\nu(t)$ exponentially approaches its steady state value ν_{ss} [see Eq. (11)]. The effects of diffusion on the full MM mechanism give rise to various forms of power-law behavior for long times, depending on the kinetic regime under investigation. There is a large literature that has explored such effects using diverse theoretical and simulation models.[7–29] Here we present simulation results that illustrate some of the phenomena exhibited by diffusion-influenced enzyme kinetics.

One of the nontrivial effects of diffusion predicted by kinetic theory[12] to exist in MM kinetics is the existence of a peak in the product production rate $\nu(t)$ that precedes a $t^{-1/2}$ power-law decay to the steady state value, $\nu_{ss}=k_{\text{cat}}[C]_{ss}$. In Fig. 4(a), we plot $\nu(t)/\nu_{\max}=[C(t)]/[E_0]$ versus time, which displays a nonmonotonic power-law approach to the steady state, in accord with earlier theoretical predictions[12] and simulations.[18]

The existence of two dynamic regimes can be discerned from the plots of $\nu(t)/\nu_{\max}$ in Fig. 4(b): a short-time regime that precedes the maximum in the plot, and a long-time regime where $\nu(t)$ decays to its steady state value. In the initial regime, abundant surrounding substrate molecules react rapidly with the enzyme and diffusion plays a minor role. In this "quasiclassical" regime, characterized by the intrinsic rate constants k^0_1 and k^0_{-1}, $\nu(t)$ increases exponentially with time constant $\tau_0=(k^0_1[S_0]+k^0_{-1}+k_{\text{cat}})^{-1}$, to an apparent intrinsic steady state value ν^0_{ss}. We denote the time at which $\nu(t)/\nu_{\max}$ deviates from $\nu^0(t)/\nu_{\max}$ by t_c. For the conditions in Fig. 4, we have $\tau_0 \ll t_c$.

In the second "diffusion-controlled" regime, diffusion dominates. In Fig. 4(b), for times longer than t_c, one sees that the system slowly relaxes to the steady state value. Since $\nu(t)/\nu_{\max}$ has exceeded its steady state value at the end of the quasiclassical regime at t_c, a peak is observed in the curve. In the diffusion-controlled regime, the rate constants attain their full values k_1 and k_{-1}. The effects of diffusion manifest themselves in the steady state values of the product production rates which satisfy the inequalities: $\nu^0_{ss}/\nu_{\max} > \nu_{ss}/\nu_{\max} > \nu^D_{ss}/\nu_{\max}$[12] [see Fig. 4(b)]. The product production rate approaches its steady state value from above, which has been also observed in recent studies.[19] Diffusion is also responsible for the slow power-law approach to the steady state. In Fig. 4(c), we show a log–log plot of the deviation $(\nu(t)-\nu_{ss})/\nu_{\max}$ in the diffusion-controlled regime, which shows the $t^{-1/2}$ asymptotic power-law behavior predicted by kinetic theory.[12]

Figure 5(a) shows results for a different set of parameters with a smaller rate constant k_{cat} and ten times smaller initial substrate concentration. Both of these changes increase the characteristic time τ_0. Now τ_0 is comparable to t_c so that the diffusion-controlled regime is reached before $\nu^0(t)$ has evolved to its peak value, ν_P. In this diffusion-influenced regime between τ_0 and the peak, a $t^{-3/2}$ power law is found, which can be seen from the log–log plot shown in Fig. 5(b). Subsequent to the formation of a very small and broad peak at ν_P, $\nu(t)$ relaxes to its steady state value with a $t^{-1/2}$ power law decay as shown in Fig. 5(c).

In addition to the kinetic theory prediction of a $t^{-1/2}$ power-law decay for $[C(t)]$ when $[S_0] \gg [E_0]$, kinetic theory also predicts[12] a $t^{-3/2}$ power law for low substrate concentrations, which depends on the initial conditions. While the parameter values and initial conditions are not the same as in the kinetic theory calculations, the results in Figs. 5(b) and 5(c) demonstrate that regimes where both $t^{-1/2}$ and $t^{-3/2}$ power-law behaviors exist for enzyme kinetics.

The $t^{-3/2}$ asymptotic behavior is the same as that for the reversible formation and dissociation of the complex, $E+S \rightleftharpoons C$. We have carried out simulations of this reversible

reaction mechanism and have confirmed the existence of a $t^{-3/2}$ power-law decay. We note that the asymptotic behavior of the reaction $E + S \rightleftharpoons C \rightleftharpoons E + P$ also shows a $t^{-3/2}$ power-law decay.[11]

In classical MM kinetics, diffusion is assumed to be fast enough so that the solution is well mixed and the depletion of substrates near the enzyme as a result of reaction may be ignored. However, this approximation is not valid in general and inhomogeneities may develop in the system that will influence the dynamics. In Fig. 6, we show the time dependent substrate–enzyme(complex) average radial distribution function,

$$g_S(r,t) = \frac{\left\langle \sum_{i=1}^{N_S(t)} \delta(r - |\mathbf{r}_{Si}(t) - \mathbf{r}_{\alpha j}(t)|) \right\rangle}{(4\pi r^2 [S(t)])}, \tag{14}$$

where $\alpha = E, C$ and the bracket signifies an average over enzymes and complexes. In Fig. 6(a), we plot the time average of $g_S(r,t)$ in the steady state. The substrate concentration gradient which is formed near the enzymes and complexes can be seen in this figure.

In dilute systems with small binding rates, similar dynamical behavior occurs near to and far from the enzyme. The concentration of substrate decreases with time as a result of product formation. If the binding reaction is fast and/or $[S_0] \gg [E_0]$, the kinetics may differ in these spatial regions. Figure 6(b) plots the time dependent substrate distribution near the enzyme divided by its value at $t = 0$. Due to the high initial concentration of substrates and fast binding to enzymes, there is strong substrate depletion at short times. Slow diffusion is unable to compensate the decrease in substrate in the binding reaction. Subsequently, some substrate molecules are released when the complex dissociates. This, in addition to replenishment by diffusion, leads to an increase and peak in the substrate concentration at intermediate times. Since products are created continuously, the substrate distribution relaxes to a quasisteady value and slowly decays to zero. These results are consistent with recent Brownian dynamics simulation studies.[19]

IV. MANY-BODY EFFECTS IN ENZYME KINETICS

Thus far we have considered systems with low concentrations of enzymes where the enzyme molecules act almost independently. Even in simple catalytic reactions, cooperative effects due to high concentrations of catalysts have been shown to lead to nonanalytic dependence of reaction rates on the volume fractions of catalytic particles.[42,48,49] If the enzymes occupy significant volume fractions of the system and no longer act independently, we expect cooperative effects to play a role; for example, substrate or product molecules which are released when the complex dissociates may diffuse through the solution and rebind to other enzymes. *In vivo* enzymatic reactions occur in crowded cellular environments where the equilibrium and and dynamical properties may be very different from their ideal solution counterparts.[50–53] Cooperative effects in systems of this type can influence catalytic turnover cycles in the system. In addition, the concentration of reactants in the vicinity of one enzyme may be affected by the presence nearby enzymes, which gives rise to spatiotemporal fluctuations and correlations between enzymes. In such cases enzyme kinetics may not be described accurately by mean field equations which neglect such correlations. In this section, we explore some features of cooperative enzyme kinetics.

A. Rate coefficients

The functional dependence of the forward and reverse reaction rates on the chemical concentrations defines the reaction rate coefficients that characterize the individual steps in a reaction mechanism. These rate coefficients are usually determined by writing the time rate of change of chemical concentrations as mass action chemical rate laws. For nonideal systems, the functional form of this relation has been the subject of considerable discussion.[54] Here we assume mass action kinetics applies and study the nature of the rate coefficients defined in this way for systems where the volume fraction of enzymes and enzyme–substrate complexes is large and the solution no longer behaves ideally. The volume fraction of enzymes and complexes is given approximately by $\phi = N_E(0)V_E/V$ since the enzymes and substrates have the same volumes V_E in our model and the total number of enzymes and complexes is conserved, $N_E(t) + N_C(t) = N_E(0)$. (For our soft potential model the volume V_E is not strictly determined but can be estimated from σ_E in the LJ potential.)

Consider the reversible binding of the substrate to the enzyme, $E + S \rightleftharpoons C$. If $\mathcal{N}_f(t)$ is the number of reactions per unit volume that convert reactants to products in the time interval t, we define the time dependent forward reaction rate by $\mathcal{R}_f(t) = d\mathcal{N}_f(t)/dt$. The reverse reaction rate is defined in an analogous fashion as $\mathcal{R}_r(t) = d\mathcal{N}_r(t)/dt$. The net reaction rate is $\mathcal{R}(t) = \mathcal{R}_f(t) - \mathcal{R}_r(t)$. The reaction rates are written in mass action form as

$$\begin{aligned} \mathcal{R}_f(t) &= k_1'(\phi,t)[E(t)][S(t)], \\ \mathcal{R}_r(t) &= k_{-1}'(\phi,t)[C(t)], \end{aligned} \tag{15}$$

where the primes denote the effective rate coefficients defined by these equations that may depend on the volume fraction as well as the time.

At equilibrium we have $\mathcal{R}_f = \mathcal{R}_r$, so that

$$\frac{[C]_{\rm eq}}{[E]_{\rm eq}[S]_{\rm eq}} = \frac{k_1'(\phi)}{k_{-1}'(\phi)}, \tag{16}$$

where the eq subscripts denote equilibrium concentrations, and rate coefficients without time arguments are the values these quantities take at equilibrium. The equilibrium constant for a nonideal system is expressed in terms of the ratio of activities as

$$K_{\rm eq} = \frac{a_C}{a_E a_S} = \frac{\gamma_C}{\gamma_E \gamma_S} \frac{[C]_{\rm eq}}{[E]_{\rm eq}[S]_{\rm eq}}, \tag{17}$$

where a_α is the activity of species α. In the second equality we used the relation between activities and concentrations $a_\alpha = \gamma_\alpha [\alpha]_{\rm eq}$ in terms of the activity coefficient γ_α. Consequently, we may write

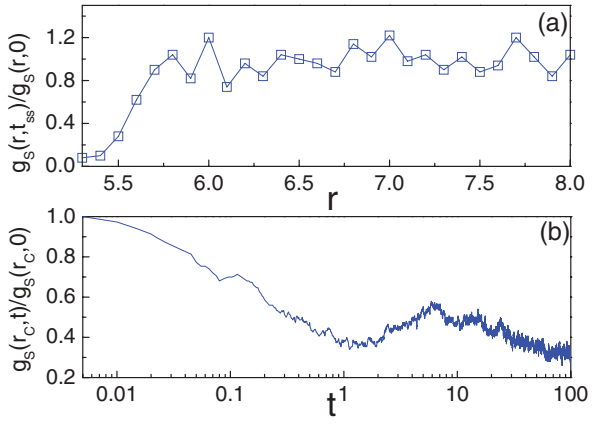

FIG. 6. (a) The normalized substrate–enzyme (complex) radial distribution function in the steady state. (b) Plot of $g_S(r_c,t)/g_S(r_c,0)$ the time dependent averaged deviation of substrate concentration at r_c. Simulation parameters: $N_E(0)=50$, $N_S(0)=10000$, $k_BT=0.05$, $\sigma_E=5.0$, $p_R=1.0$, $k_{-1}^0=5.0$, and $k_{\rm cat}=0.5$.

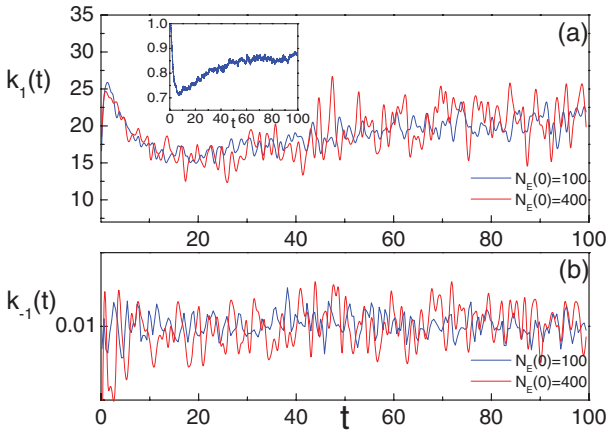

FIG. 7. Time dependent rate coefficients in the reversible reaction $E+S \rightleftharpoons C$ for different initial numbers of enzyme molecules. (a) The time evolution of $k_1(t)$. Inset: plot of $g_S(r_c,t)/g_S(r_c,0)$ (ordinate), the time dependent substrate radial distribution function at r_c, vs time (abscissa). (b) The time evolution of $k_{-1}(t)$. Simulation parameters: $N_S(0)=1000$, $k_BT=0.2$, $\sigma_E=3.0$, $p_R=1.0$, and $k_{-1}=0.01$. The data are the result of an average over 64 realizations with different initial random configurations of enzymes.

$$K_{\rm eq}=\frac{\gamma_C}{\gamma_E\gamma_S}\frac{k_1'(\phi)}{k_{-1}'(\phi)}. \tag{18}$$

This equation provides a relation between the ratio of effective forward and reverse rate coefficients and the equilibrium constant in the nonideal system.

Simulations of the enzyme reaction dynamics for systems with large ϕ can be used to explore if a mass action description is the most appropriate or convenient way to analyze the kinetics. For our model system, the relation between the activity and concentration is largely determined by volume exclusion effects. Approximating the enzymes and complexes as hard spherical particles, the activity coefficient of species α is given by[51] $\gamma_\alpha=1/p_\alpha$, where p_α is the probability of successful insertion of a molecule of species α at a random location in the system. For the point substrate particles, this is just fraction of the total volume not occupied by enzymes or complexes, $p_S=1-\phi$, so $\gamma_S=1/(1-\phi)$. Similar considerations apply for γ_E and γ_C but one must account for the finite sizes of these species; however, since the volume of an enzyme is the same as that of a complex, $\gamma_E=\gamma_C$. Hence, we have the more specific relation between the equilibrium constant and the effective rate coefficients,

$$K_{\rm eq}=\frac{k_1'(\phi)(1-\phi)}{k_{-1}'(\phi)}. \tag{19}$$

The forward and reverse rate coefficients were determined from the simulations using the definitions discussed above. The results show that $k_{-1}'(\phi,t)$ is weakly dependent on ϕ and the results for different ϕ cannot be distinguished within the statistical uncertainty of our simulations; however, $k_1'(\phi,t)$ depends strongly on the enzyme and complex volume fraction, in accord with earlier observations.[28]

In view of these results and Eq. (19), it is convenient to scale k_1' by $(1-\phi)$ and define the scaled forward, $k_1(t)\equiv k_1'(\phi)(1-\phi)$, and reverse, $k_{-1}(t)\equiv k_{-1}'(\phi)$, rate coefficients. Figure 7 plots the $k_1(t)$ and $k_{-1}(t)$ rate coefficients versus time for two different initial numbers of enzyme molecules: $N_E(0)=100$ corresponding to a system with a small enzyme volume fraction ($\phi\approx 0.074$), and $N_E(0)=400$, where $\phi\approx 0.29$. We observe that $k_1(t)$ is independent of ϕ within the statistical uncertainty of our simulations, so we have omitted the ϕ dependence of $k_1(t)$ and $k_{-1}(t)$ in our notation; however, we cannot rule out a weak dependence on ϕ. These results suggest that proposals that relate the reaction rate to expressions involving the activities[54,55] may provide a convenient way to analyze rate data.

The rate coefficient $k_1(t)$ displayed in Fig. 7 evolves to its asymptotic value in a nonmonotonic fashion.[56] The inset of Fig. 7(a) shows the time dependent substrate radial distribution function near the enzyme. The features that are responsible for the structure of $g_S(r_c,t)/g_S(r_c,0)$ were discussed earlier in connection with the plot in Fig. 6. Here, however, no product molecules are produced in the reaction. In this case, the substrate molecules which are released when the complex dissociates, along with the substrate molecules that arrive by diffusion, gradually increase the local substrate concentration near the enzyme, after the initial fast substrate depletion due to the complex formation reaction. This effect is responsible for the nonmonotonic time evolution of $k_1(t)$.

We can contrast this situation with that for irreversible reactions leading to the formation of the complex. We consider the reaction $E+S\rightarrow C\rightarrow E+P$ where substrates are completely converted to products with no substrate release. Figure 8 plots the time dependent rate coefficient $k_1(t)$ for two different initial numbers of enzymes. Again, these scaled rate coefficients exhibit data collapse for different ϕ values.

The continuous conversion of $S\rightarrow P$ leads to a reduction of $g_S(r_c,t)/g_S(r_c,0)$ near the enzyme. From the right inset in Fig. 8, one can see that a strong substrate concentration gradient develops near the enzyme. The value of k_1^0 obtained from $k_1(t=0)$ in the simulation is in accord with the estimate of the intrinsic rate constant using Eq. (13), $k_1^0\approx 25.3$.

The steady state rate constant k_1 can be determined from the long time value of $k_1(t)$. From Fig. 8 (left inset) we see

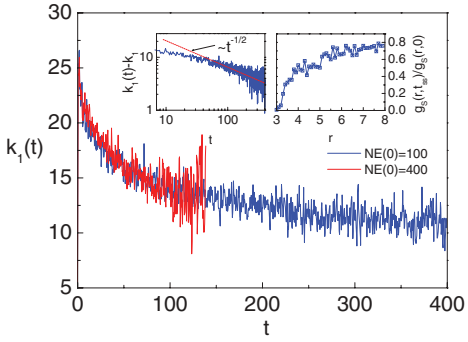

FIG. 8. Time dependent rate coefficients $k_1(t)$ in the reaction $E + S \to C \to E + P$. Left inset: Log–log plot of $k_1(t) - k_1$ and fit (red dotted line) to a power law, $t^{-1/2}$ for long times. Right inset: the substrate–enzyme (complex) radial distribution function in the steady state. Simulation parameters: $N_S(0) = 100$, $N_S(0) = 5000$, $k_BT = 0.2$, $\sigma_E = 3.0$, $p_R = 1.0$, and $k_{\rm cat} = 0.5$. The data are the result of an average over 64 realizations with different initial random configurations of enzymes.

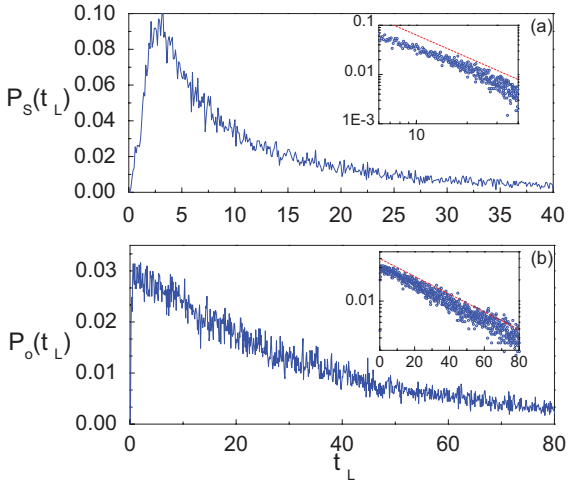

FIG. 9. (a) Lifetime distribution for rebinding to the same enzyme. Inset: Log–log plot and fit (red dotted line) showing the $t^{-3/2}$ power-law decay. (b) Lifetime distribution for rebinding to other enzymes. Inset: Linear-log plot and fit (red dotted line) to an exponential decay, $e^{-t_L/33.3}$. Simulation parameters: $N_E(0) = 400$, $N_S(0) = 5000$, $k_BT = 0.2$, $\sigma_E = 3.0$, $p_R = 1.0$, $k_{-1}^0 = 0.5$, and $k_{\rm cat} = 0.05$. The data are an average of 32 realizations of the dynamics.

that $k_1(t)$ decays monotonically as a $t^{-1/2}$ power law to its steady state value, in accord with the asymptotic form of Eq. (12),

$$k_1(t) \sim \frac{k_1^0 k_D}{k_1^0 + k_D}\left[1 + \frac{k_1^0 \bar{\sigma}_E}{k_1^0 + k_D}(\pi D t)^{-1/2}\right]. \tag{20}$$

The predicted steady state rate coefficient is $k_1 = k_1^0 k_D/(k_1^0 + k_D)$. We can estimate k_D from the known value of the diffusion coefficient $D = D_E + D_S \approx D_S = 0.24$, where we have used the analytical expression for the diffusion coefficient for MPC dynamics,[37]

$$D_S = \frac{k_BT\tau}{2m}\left(\frac{3\gamma}{(\gamma - 1 + e^{-\gamma})(1 - \cos\alpha)} - 1\right), \tag{21}$$

where γ is the number of particles per MPC cell. We find $k_D = 10.1$, which yields $k_1 = 7.2$. Determining k_1 from an extrapolation of the simulation data, we find $k_1 \approx 7.4$ which is consistent with the theoretical estimate.

B. Lifetime distributions

In order to provide additional details on many-body enzyme effects in the substrate binding processes, we computed statistics related to the fates of substrate molecules that are formed when a complex dissociates. A newly released substrate molecule may rebind to the same enzyme from which it was released, bind to another enzyme in the system or, in an infinite system, remain unbound.

The lifetime distributions of the newly released substrate molecules can be computed by recording the time intervals t_L between the release of a substrate molecule and its subsequent rebinding, either to the same or different enzyme molecules. We denote by $P_s(t_L)$ and $P_o(t_L)$ the lifetime probability densities for rebinding to the same and different enzymes, respectively. In Fig. 9(a), we see that $P_s(t_L)$ decays with a $t_L^{-3/2}$ power law as expected for a diffusive process.[57,58] The distribution $P_o(t_L)$ exhibits an exponential decay e^{-t_L/τ_L} with characteristic time $\tau_L = 33.3$ for the chosen simulation parameters. The time τ_L depends on the average distance ℓ_E between enzyme molecules, which varies in time as the reaction proceeds. An order of magnitude estimate of the decay time is $\tau_L \sim \ell_E^2/6D$. If the average number of enzyme molecules in the system after a rapid initial decay, $\bar{N}_E \approx 225$, is used to estimate $\ell_E \approx (V/\bar{N}_E)^{1/3} - 2r_c \approx 3.1$ ($2r_c$ is subtracted to account for the finite sizes of the enzymes), we obtain $\tau_L \approx 6.6$.

The binding of substrate molecules to enzymes that are different from those from which they were released can lead to cooperative enzyme many-body effects, such as the synchronous operation of ensembles of enzymes. In addition studies of the type described above can be extended to consider cases where the products produced by one type of enzyme can act as inhibitors or substrates for different types of enzymes in the system, resulting in more complicated kinetics.

V. CONCLUSION

The mesoscopic model described in this paper provides a basis for a simulation scheme that can be used to study a variety of features related to the effects of diffusion, reaction, and hydrodynamics on enzyme kinetics. A coarse grained description is adopted where the enzyme is modeled as a finite-size spherical particle and its reactive and nonreactive dynamics with substrate molecules account for basic properties of the dynamics. While all details related to specific aspects of substrate binding and unbinding, the reactive event leading to product formation, and possible conformational changes in the enzyme during the catalytic process are subsumed in the rates of simple reactive and nonreactive collision events, the model preserves a number of important features that are essential for a proper description of the dynamics at a coarse grained level. The model is particle-based and includes enzyme, substrate, enzyme–substrate complex, product, and solvent molecules. The collision dynamics is constructed to sat-

isfy mass, momentum, and energy conservation laws. Since the dynamics involves complex formation and dissociation, the solvent plays a crucial role in preserving energy and momentum conservation. Since all of these conservation laws are satisfied, in particular momentum conservation, hydrodynamic interactions among the enzymes and complexes is taken into account in the dynamics.

The influence of diffusion on the enzyme kinetics was explored and a variety of different power-law regimes, as well as regimes where both nonmonotonic and monotonic evolution of the product production rate to its steady state value, were observed in accord with earlier investigations using different theoretical and simulation methods. For systems where the enzymes occupy significant volume fractions of the system, the structure of the chemical rate law and the forms of the time and volume-fraction-dependent rate coefficients that characterize the reactive dynamics were explored. A formulation of the rate law in terms of activities provided a useful way to analyze the simulation results.

The model could be used to explore a variety of problems in this area. Applications involving cooperative enzyme dynamics may be difficult to study by other means; however, since all species, including solvent, are treated in the dynamical model, diffusive and hydrodynamic collective motions are taken into account without the need for the introduction of phenomenological space and time dependent transport properties. The model may also be generalized to include finer detail in the enzyme conformational structure and dynamics.

ACKNOWLEDGMENTS

This work was supported in part by a grant from the Natural Sciences and Engineering Council of Canada.

APPENDIX: CONSTRUCTION OF REACTIVE COLLISION DYNAMICS

1. The reaction $A + B \to C$

We consider a general binary reaction between species A and B that leads to the formation of the complex C. Once an AB pair with relative separation, $r_{AB} = |\mathbf{r}_A - \mathbf{r}_B| \le r_c$, in the reaction zone is selected for reaction, the complex C is formed with mass $m_C = m_{AB} = m_A + m_B$ to ensure mass conservation. We also require that momentum and energy be conserved. Before the reactive event the total momentum of the colliding A and B particles is $\mathbf{p}_A + \mathbf{p}_B = \mathbf{P}_{AB} = m_{AB}\mathbf{V}_{AB}$, where the center of mass velocity of the pair is $\mathbf{V}_{AB} = (m_A\mathbf{v}_A + m_B\mathbf{v}_B)/m_{AB}$. To conserve momentum in this reactive event, we choose the momentum of the newly formed complex, $\mathbf{p}'_C$, to be equal to the total momentum of the AB pair before reaction: $\mathbf{p}'_C = \mathbf{P}_{AB}$. In terms of velocities we have $\mathbf{v}'_C = \mathbf{V}_{AB}$.

The total energy of the pair before reaction is

$$\begin{aligned}&\tfrac{1}{2}m_A v_A^2 + \tfrac{1}{2}m_B v_B^2 + \mathcal{V}_{AB}(r_{AB})\\ &\quad = \tfrac{1}{2}\mu_{AB}v_r^2 + \tfrac{1}{2}m_{AB}V_{AB}^2 + \mathcal{V}_{AB}(r_{AB}).\end{aligned} \tag{A1}$$

In the right equality, we have written the total kinetic energy in terms of the relative and center of mass kinetic energies of the pair. Here $\mathcal{V}_{AB}(r_{AB})$ is the $A-B$ pair potential and $\mu_{AB} = m_A m_B/m_{AB}$ the reduced mass. Since $\mathbf{v}'_C = \mathbf{V}_{AB}$ from momentum conservation, the kinetic energy of the complex that is formed on reaction is $1/2m_C v_C'^2 = 1/2m_{AB}V_{AB}^2$, consequently we must dispose of the kinetic and potential energy of the relative motion of the AB pair in order to conserve energy. We can do this by allowing energy to flow into the solvent. In particular if there are n solvent molecules in the vicinity of the reactive AB pair, we can adjust the velocities of these solvent molecules to account for the AB relative energy. Thus, accounting for these neighboring solvent molecules, total energy conservation in the reaction reads

$$\begin{aligned}&\frac{1}{2}\mu_{AB}v_r^2 + \frac{1}{2}m_{AB}V_{AB}^2 + \mathcal{V}_{AB}(r_{AB})\\ &\quad + \sum_{j=1}^{n}\frac{1}{2}m_M v_{Mj}^2 + \sum_{j=1}^{n}\mathcal{V}_{Aj}(r_{Aj})\\ &\qquad = \frac{1}{2}m_C v_C'^2 + \sum_{j}^{n}\frac{1}{2}m_M v_{Mj}'^2 + \sum_{j}^{n}\mathcal{V}_{Aj}(r_{Aj}),\end{aligned} \tag{A2}$$

where the primes again denote postcollision quantities. Since the r_{Aj} distances do not change on reaction and $1/2m_C v_C'^2 = 1/2m_{AB}V_{AB}^2$ as noted above, this equation simplifies to

$$\frac{1}{2}\mu_{AB}v_r^2 + \mathcal{V}_{AB}(r_{AB}) + \sum_{j=1}^{n}\frac{1}{2}m_M v_{Mj}^2 = \sum_{j}^{n}\frac{1}{2}m_M v_{Mj}'^2. \tag{A3}$$

Of course the total momentum of these participating solvent molecules must also be conserved so that

$$\sum_{j=1}^{n}\mathbf{p}_{Mj} = \sum_{j=1}^{n}\mathbf{p}'_{Mj}, \tag{A4}$$

which is equivalent to requiring that the precollision and postcollision center of mass velocities of the n solvent molecules are the same: $1/n\sum_{j=1}^{n}\mathbf{V}_{Mj} = \mathbf{V}_M^{(n)} = \mathbf{V}_M^{(n)\prime}$.

These relations allow the postreaction velocities of the participating solvent molecules to be determined. In view of the fact that $\mathbf{V}_M^{(n)} = \mathbf{V}_M^{(n)\prime}$, Eq. (A3) can be written in terms of solvent velocities relative to their center of mass as

$$\begin{aligned}&\sum_{j}^{n}\frac{1}{2}m_M\left(\mathbf{v}'_{Mj} - \mathbf{V}_M^{(n)}\right)^2\\ &\quad = \frac{1}{2}\mu_{AB}v_r^2 + \mathcal{V}_{AB}(r_{AB}) + \sum_{j=1}^{n}\frac{1}{2}m_M\left(\mathbf{v}_{Mj} - \mathbf{V}_M^{(n)}\right)^2.\end{aligned} \tag{A5}$$

Partitioning the AB pair relative energy equally among the n solvent molecules, we may solve for the magnitude of the postreaction solvent velocities, relative to their center of mass velocity to obtain

$$\begin{aligned}\left|\mathbf{v}'_{Mj} - \mathbf{V}_M^{(n)}\right| = \Big[&\frac{\mu_{AB}}{nm_M}v_r^2 + \frac{2}{nm_M}\mathcal{V}_{AB}(r_{AB})\\ &+ (\mathbf{v}_{Mj} - \mathbf{V}_M^{(n)})^2\Big]^{1/2}.\end{aligned} \tag{A6}$$

It remains to specify the unit vectors $\hat{\mathbf{n}}_j$ that determine the directions of the solvent relative velocities. There is considerable freedom in how this can be done. Since we must satisfy $\sum_j^n \left(\mathbf{v}'_{Mj} - \mathbf{V}_M^{(n)}\right) = 0$, one way is to simply choose the unit vectors of $n-1$ participating solvent molecules at random. The remaining unit vector, say $\hat{\mathbf{n}}_n$, is then determined by the condition,

$$\hat{\mathbf{n}}_n = -\sum_j^{n-1} \hat{\mathbf{n}}_j \frac{\left|\mathbf{v}'_{Mj} - \mathbf{V}_M^{(n)}\right|}{\left|\mathbf{v}'_{Mn} - \mathbf{V}_M^{(n)}\right|}. \tag{A7}$$

The postreaction values of the velocities of the participating solvent particles are then given by

$$\mathbf{v}'_{Mj} = \mathbf{V}_M^{(n)} + \hat{\mathbf{n}}_j \left|\mathbf{v}'_{Mj} - \mathbf{V}_M^{(n)}\right|, \quad j = 1, \ldots, n, \tag{A8}$$

with $|\mathbf{v}'_{Mj} - \mathbf{V}_M^{(n)}|$ given by Eq. (A6). Equation (A8), along with $\mathbf{v}'_C = \mathbf{V}_{AB}$, completely determines the postreaction solvent and enzyme–substrate-complex velocities so that mass, momentum and energy are conserved.

As an illustration of these general formulas, consider the case where two solvent molecules ($n = 2$) participate in the energy exchange on reaction. For $n = 2$, Eq. (A6) reads

$$v'_{Mr} = \left(\frac{2\mu_{AB}}{m_M} v_r^2 + \frac{4}{m_M}\mathcal{V}_{AB}(r_{AB}) + v_{Mr}^2\right)^{1/2}, \tag{A9}$$

where $\mathbf{v}_{Mr} = \mathbf{v}_{M1} - \mathbf{v}_{M2}$. Equation (A7) gives $\hat{\mathbf{n}}_2 = -\hat{\mathbf{n}}_1$, where $\hat{\mathbf{n}}_1$ is a randomly chosen unit vector and from Eq. (A8) the postreaction solvent velocities are

$$\begin{aligned} \mathbf{v}'_{M1} &= \mathbf{V}_M^{(2)} + \tfrac{1}{2}\hat{\mathbf{n}}_1 v'_{Mr} \\ \mathbf{v}'_{M2} &= \mathbf{V}_M^{(2)} - \tfrac{1}{2}\hat{\mathbf{n}}_1 v'_{Mr}. \end{aligned} \tag{A10}$$

These expressions are used in the simulations described in the text.

2. The reaction $C \rightarrow A + B$

The postreaction velocities for the reaction $C \rightarrow A + B$ can be computed in the following way so as to satisfy mass, momentum, and energy conservations. Mass conservation of course requires that $m_C = m_A + m_B$, while momentum conservation implies that

$$m_C \mathbf{v}_C = m_A \mathbf{v}'_A + m_B \mathbf{v}'_B = m_C \mathbf{V}'_{AB}, \tag{A11}$$

or $\mathbf{v}_C = \mathbf{V}'_{AB}$. If we just consider the A, B, and C species, energy conservation gives

$$\begin{aligned} \tfrac{1}{2} m_C v_C^2 &= \tfrac{1}{2} m_A v_A'^2 + \tfrac{1}{2} m_B v_B'^2 + \mathcal{V}_{AB}(r_{AB}) \\ &= \tfrac{1}{2}\mu_{AB} v_r'^2 + \tfrac{1}{2} m_C V_{AB}'^2 + \mathcal{V}_{AB}(r_{AB}), \end{aligned} \tag{A12}$$

which, in view of momentum conservation, would put a severe restriction on v'_r that cannot always be satisfied. Once again we need to utilize the presence of surrounding solvent molecules to provide energy to the newly formed A and B molecules for them to separate. Taking into account the presence of n neighboring solvent molecules, energy conservation now becomes

$$\begin{aligned} &\frac{1}{2} m_C v_C^2 + \sum_j^n \frac{1}{2} m_M v_{Mj}^2 \\ &= \frac{1}{2}\mu_{AB} v_r'^2 + \frac{1}{2} m_C V_{AB}'^2 + \mathcal{V}_{AB}(r_{AB}) + \sum_j^n \frac{1}{2} m_M v_{Mj}'^2. \end{aligned} \tag{A13}$$

Momentum conservation for these participating solvent molecules implies that $\mathbf{V}_M^{(n)} = \mathbf{V}_M^{(n)\prime}$. Taking into account momentum conservation for all species participating in the reaction, the energy conservation condition becomes

$$\begin{aligned} &\sum_j^n \frac{1}{2} m_M \left(\mathbf{v}_{Mj} - \mathbf{V}_M^{(n)}\right)^2 \\ &= \frac{1}{2}\mu_{AB} v_r'^2 + \mathcal{V}_{AB}(r_{AB}) + \sum_j^n \frac{1}{2} m_M \left(\mathbf{v}'_{Mj} - \mathbf{V}_M^{(n)}\right)^2. \end{aligned} \tag{A14}$$

Thus, the magnitude of the postreaction relative velocity is given by

$$\begin{aligned} v'_r = \Big[&- \frac{2}{\mu_{AB}} \mathcal{V}_{AB}(r_{AB}) \\ &+ \frac{m_M}{\mu_{AB}} \sum_j^n \left(\left(\mathbf{v}_{Mj} - \mathbf{V}_M^{(n)}\right)^2 - \left(\mathbf{v}'_{Mj} - \mathbf{V}_M^{(n)}\right)^2 \right) \Big]^{1/2}. \end{aligned} \tag{A15}$$

Once the postreaction values of the velocities of the participating solvent molecules are specified, the above equation determines v'_r. The direction of $\mathbf{v}'_r$ can be chosen to be in the outward radial direction from A to B, $\hat{\mathbf{r}}_{BA}$. A convenient choice for the $\mathbf{v}'_{Mj}$ follows from the assumption that postreaction velocities, relative to their center of mass velocity, are zero so that their relative energies are converted into relative energy of the newly formed A and B molecules. Thus, $\mathbf{v}'_{Mj} = \mathbf{V}_M^{(n)}$ and

$$v'_r = \Big[- \frac{2}{\mu_{AB}} \mathcal{V}_{AB}(r_{AB}) + \frac{m_M}{\mu_{AB}} \sum_j^n \left(\mathbf{v}_{Mj} - \mathbf{V}_M^{(n)}\right)^2 \Big]^{1/2}. \tag{A16}$$

Again, consider the case where only two neighboring solvent molecules provide the thermal energy and the newly created S or P molecule lies outside the range of the AB potential so that $\mathcal{V}_{AB}(r_{AB}) = 0$. In this case, Eq. (A16) takes the form,

$$v'_r = \sqrt{\frac{m_M}{2\mu_{AB}}} |\mathbf{v}_{M1} - \mathbf{v}_{M2}|, \tag{A17}$$

and

$$\begin{aligned} \mathbf{v}'_A &= \mathbf{v}_C + \frac{m_B}{m_C} \sqrt{\frac{m_M}{2\mu_{AB}}} \hat{\mathbf{r}}_{BA} |\mathbf{v}_{M1} - \mathbf{v}_{M2}|, \\ \mathbf{v}'_B &= \mathbf{v}_C - \frac{m_A}{m_C} \sqrt{\frac{m_M}{2\mu_{AB}}} \hat{\mathbf{r}}_{BA} |\mathbf{v}_{M1} - \mathbf{v}_{M2}|. \end{aligned} \tag{A18}$$

[1] L. Michaelis and M. L. Menten, Biochem. Z. **49**, 333 (1913).
[2] M. von Smoluchowski, Ann. Phys. **48**, 1003 (1915); Phys. Z. **17**, 557 (1916); Z. Phys. Chem. **92**, 129 (1917).
[3] R. Kapral, Adv. Chem. Phys. **48**, 71 (1981).
[4] D. F. Calef and J. M. Deutch, Ann. Rev. Phys. Chem. **34**, 493 (1983).
[5] A. Szabo, J. Phys. Chem. **93**, 6929 (1989).
[6] V. Casagrande, Y. Togashi, and A. S. Mikhailov, Phys. Rev. Lett. **99**, 048301 (2007).
[7] Ya. B. Zeldovich and A. A. Ovchinnikov, JETP Lett. **26**, 440 (1977).
[8] I. V. Gopich and N. Agmon, Phys. Rev. Lett. **84**, 2732 (2000).
[9] I. V. Gopich, A. A. Ovchinnikov, and A. Szabo, Phys. Rev. Lett. **86**, 2732 (2001).
[10] H. Kim and K. J. Shin, Phys. Rev. Lett. **82**, 1578 (1999).
[11] S. Paul and G. Gangopadhyay, J. Chem. Phys. **119**, 3501 (2003).
[12] H. Kim, M. Yang, M. Choi, and K. J. Shin, J. Chem. Phys. **115**, 1455 (2001).
[13] H. Kim and K. J. Shin, J. Phys.: Condens. Matter **19**, 065137 (2007).
[14] S. Lee and M. Karplus, J. Chem. Phys. **83**, 1883 (1987).
[15] N. Agmon and A. Szabo, J. Chem. Phys. **92**, 5270 (1990).
[16] G. Oshnin, O. Benichou, M. Coppey, and M. Moreau, Phys. Rev. E **66**, 060101(R) (2002).
[17] A. Szabo, J. Chem. Phys. **95**, 2481 (1991).
[18] S. Park and N. Agmon, J. Phys. Chem. B **112**, 5977 (2008).
[19] S. Park and N. Agmon, J. Phys. Chem. B **112**, 12104 (2008).
[20] H. Zhou, J. Phys. Chem. B **101**, 6642 (1997).
[21] H. X. Zhou and A. Szabo, Biophys. J. **71**, 2440 (1996).
[22] R. Murugan, J. Chem. Phys. **117**, 4178 (2002).
[23] B. J. Sung and A. Yethiraj, J. Chem. Phys. **123**, 114503 (2005).
[24] A. V. Popov and N. Agmon, Chem. Phys. Lett. **340**, 151 (2001).
[25] H. Kim, M. Yang, and K. J. Shin, J. Chem. Phys. **11**, 1068 (1999).
[26] M. Litniewski, J. Chem. Phys. **123**, 124506 (2005); **125**, 174501 (2006).
[27] M. Litniewski, Acta Phys. Pol. B **39**, 1161 (2008).
[28] H. Berry, Biophys. J. **83**, 1891 (2002).
[29] D. Barik, M. R. Paul, W. T. Baumann, Y. Cao, and J. J. Tyson, Biophys. J. **95**, 3563 (2008).
[30] D. Huppert, S. Y. Goldberg, A. Masad, and N. Agmon, Phys. Rev. Lett. **68**, 3932 (1992).
[31] K. M. Solntsev, D. Huppert, and N. Agmon, Phys. Rev. Lett. **86**, 3427 (2001).
[32] D. Pines and E. Pines, J. Chem. Phys. **115**, 951 (2001).
[33] K. M. Solntsev, D. Huppert, and N. Agmon, J. Phys. Chem. A **105**, 5868 (2001).
[34] S. Allison, J. Phys. Chem. A **110**, 13864 (2006).
[35] A. Malevanets and R. Kapral, J. Chem. Phys. **110**, 8605 (1999).
[36] A. Malevanets and R. Kapral, J. Chem. Phys. **112**, 7260 (2000).
[37] R. Kapral, Adv. Chem. Phys. **140**, 89 (2008).
[38] G. Gompper, T. Ihle, D. M. Kroll, and R. G. Winkler, Adv. Polym. Sci. **221**, 1 (2009).
[39] T. Ihle and D. Kroll, Phys. Rev. E **67**, 066706 (2003); E. Tuzel, M. Strauss, T. Ihle, and D. Kroll, Phys. Rev. E **68**, 036701 (2003); T. Ihle, E. Tuzel, and D. Kroll, Phys. Rev. E **72**, 046707 (2005).
[40] M. Ripoll, K. Mussawisade, R. Winkler, and G. Gompper, Phys. Rev. E **72**, 016701 (2005).
[41] J. M. Yeomans, Phys. A **369**, 159 (2006); N. Kikuchi, C. M. Pooley, J. F. Ryder, and J. M. Yeomans, J. Chem. Phys. **119**, 6388 (2003); C. M. Pooley and J. M. Yeomans, J. Phys. Chem. B **109**, 6505 (2005).
[42] K. Tucci and R. Kapral, J. Chem. Phys. **120**, 8262 (2004).
[43] K. Rohlf, S. Fraser, and R. Kapral, Comp. Phys. Commun. **98**, 150603 (2008).
[44] A more detailed MD–MPC mesoscopic description of an elastic network model of an enzyme undergoing conformational changes as a result of substrate binding and product release can be found in [A. Cressman, Y. Togashi, A. Mikhailov, and R. Kapral, Phys. Rev. E **77**, 050901(R) (2008)]. This type of mesoscopic description can be extended and combined with some features of the present model to treat more realistic models of proteins.
[45] The model can be extended to account for energy changes that may accompany the catalytic conversion of $S \to P$ in the protein by associating internal energies E_S and E_P to S and P, respectively. All or a portion of the energy change in the reaction can then be deposited in the solvent, product, and enzyme molecules to be consistent with energy conservation.
[46] T. Ihle and D. M. Kroll, Phys. Rev. E **63**, 020201(R) (2001).
[47] M. Eigen, W. Kruse, G. Maass, and L. De Maeyer, Prog. React. Kinet. **2**, 287 (1964).
[48] B. U. Felderhof and J. M. Deutch, J. Chem. Phys. **64**, 4551 (1976).
[49] J. R. Lebenhaft and R. Kapral, J. Stat. Phys. **20**, 25 (1979).
[50] T. C. Laurent, Biophys. Chem. **57**, 7 (1995).
[51] S. B. Zimmerman and A. P. Minton, Annu. Rev. Biophys. Biomol. Struct. **22**, 27 (1993).
[52] A. P. Minton, J. Biol. Chem. **276**, 10577 (2001).
[53] H. X. Zhou, G. Rivas, and A. P. Minton, Annu. Rev. Biophys. **37**, 375 (2008).
[54] M. Pekar, Prog. React. Kinet. Mech. **30**, 3 (2005).
[55] R. Hasse, Z. Phys. Chem. **128**, 225 (1981).
[56] Here we are not referring to the initial value of zero and subsequent very rapid rise of $k_1(t)$ which is a consequence of the soft potential model for enzyme–substrate interactions.
[57] W. H. McCrea and F. J. Whipple, Proc. R. Soc. Edinburgh **60**, 281 (1940).
[58] P. G. Doyle and J. L. Snell, *Random Walks and Electric Networks* (Mathematical Association of America, Washington, 1984).